Study of Cabibbo Suppressed Decays of the D_s^+ Charmed-Strange Meson involving a K_S^0

The FOCUS Collaboration [1]

J. M. Link[a] P. M. Yager[a] J. C. Anjos[b] I. Bediaga[b]
C. Castromonte[b] A. A. Machado[b] J. Magnin[b] A. Massafferri[b]
J. M. de Miranda[b] I. M. Pepe[b] E. Polycarpo[b] A. C. dos Reis[b]
S. Carrillo[c] E. Casimiro[c] E. Cuautle[c] A. Sánchez-Hernández[c]
C. Uribe[c] F. Vázquez[c] L. Agostino[d] L. Cinquini[d]
J. P. Cumalat[d] V. Frisullo[d] B. O'Reilly[d] I. Segoni[d]
K. Stenson[d] R. S. Tucker[d] J. N. Butler[e] H. W. K. Cheung[e]
G. Chiodini[e] I. Gaines[e] P. H. Garbincius[e] L. A. Garren[e]
E. Gottschalk[e] P. H. Kasper[e] A. E. Kreymer[e] R. Kutschke[e]
M. Wang[e] L. Benussi[f] S. Bianco[f] F. L. Fabbri[f] A. Zallo[f]
M. Reyes[g] C. Cawlfield[h] D. Y. Kim[h] A. Rahimi[h] J. Wiss[h]
R. Gardner[i] A. Kryemadhi[i] Y. S. Chung[j] J. S. Kang[j]
B. R. Ko[j] J. W. Kwak[j] K. B. Lee[j] K. Cho[k] H. Park[k]
G. Alimonti[ℓ] S. Barberis[ℓ] M. Boschini[ℓ] A. Cerutti[ℓ]
P. D'Angelo[ℓ] M. DiCorato[ℓ] P. Dini[ℓ] L. Edera[ℓ] S. Erba[ℓ]
P. Inzani[ℓ] F. Leveraro[ℓ] S. Malvezzi[ℓ] D. Menasce[ℓ]
M. Mezzadri[ℓ] L. Moroni[ℓ] D. Pedrini[ℓ] C. Pontoglio[ℓ] F. Prelz[ℓ]
M. Rovere[ℓ] S. Sala[ℓ] T. F. Davenport III[m] V. Arena[n] G. Boca[n]
G. Bonomi[n] G. Gianini[n] G. Liguori[n] D. Lopes Pegna[n]
M. M. Merlo[n] D. Pantea[n] S. P. Ratti[n] C. Riccardi[n] P. Vitulo[n]
C. Göbel[o] J. Otalora[o] H. Hernandez[p] A. M. Lopez[p]
H. Mendez[p] A. Paris[p] J. Quinones[p] J. E. Ramirez[p] Y. Zhang[p]
J. R. Wilson[q] T. Handler[r] R. Mitchell[r] D. Engh[s] M. Hosack[s]
W. E. Johns[s] E. Luiggi[s] M. Nehring[s] P. D. Sheldon[s]
E. W. Vaandering[s] M. Webster[s] M. Sheaff[t]

[a]*University of California, Davis, CA 95616*

[b]*Centro Brasileiro de Pesquisas Físicas, Rio de Janeiro, RJ, Brazil*

[c]*CINVESTAV, 07000 México City, DF, Mexico*

^{d}*University of Colorado, Boulder, CO 80309*

^{e}*Fermi National Accelerator Laboratory, Batavia, IL 60510*

^{f}*Laboratori Nazionali di Frascati dell'INFN, Frascati, Italy I-00044*

^{g}*University of Guanajuato, 37150 Leon, Guanajuato, Mexico*

^{h}*University of Illinois, Urbana-Champaign, IL 61801*

^{i}*Indiana University, Bloomington, IN 47405*

^{j}*Korea University, Seoul, Korea 136-701*

^{k}*Kyungpook National University, Taegu, Korea 702-701*

$^{\ell}$*INFN and University of Milano, Milano, Italy*

^{m}*University of North Carolina, Asheville, NC 28804*

^{n}*Dipartimento di Fisica Nucleare e Teorica and INFN, Pavia, Italy*

^{o}*Pontifícia Universidade Católica, Rio de Janeiro, RJ, Brazil*

^{p}*University of Puerto Rico, Mayaguez, PR 00681*

^{q}*University of South Carolina, Columbia, SC 29208*

^{r}*University of Tennessee, Knoxville, TN 37996*

^{s}*Vanderbilt University, Nashville, TN 37235*

^{t}*University of Wisconsin, Madison, WI 53706*

Abstract

We study the decay of D_s^+ mesons into final states involving a K_S^0 and report the discovery of Cabibbo suppressed decay modes $D_s^+ \to K_S^0 \pi^- \pi^+ \pi^+$ (179±36 events) and $D_s^+ \to K_S^0 \pi^+$ (113±26 events). The branching ratios for the new modes are $\frac{\Gamma(D_s^+ \to K_S^0 \pi^- \pi^+ \pi^+)}{\Gamma(D_s^+ \to K_S^0 K^- \pi^+ \pi^+)} = 0.18\pm0.04\pm0.05$ and $\frac{\Gamma(D_s^+ \to K_S^0 \pi^+)}{\Gamma(D_s^+ \to K_S^0 K^+)} = 0.104\pm0.024\pm0.013$.

PACS numbers: 13.25.Ft, 14.40Lb

An essential ingredient to accurately model backgrounds in heavy quark systems involves the identification and categorization of missing decay channels in the charm sector. This is particularly important for the D_s^+ decays where a substantial part of its hadronic decay rate is yet to be identified. Only two D_s^+ Cabibbo suppressed decays have been reported, namely $D_s^+ \to K^+ \pi^+ \pi^-$ [1,2] and its resonance substructure and $D_s^+ \to K^+ K^+ K^-$ [3]. It was found that $\frac{D_s^+ \to K^+ \pi^+ \pi^-}{D_s^+ \to K^+ K^- \pi^+} = 0.127 \pm 0.007 \pm 0.014$ and $\frac{D_s^+ \to K^+ K^- K^+}{D_s^+ \to K^+ K^- \pi^+} = (8.95 \pm 2.12 ^{+2.24}_{-2.31}) \times 10^{-3}$. The two Cabibbo suppressed channels differ by an order of magnitude (partly due to phase space) and additional decays are needed to establish patterns. In this paper we report the discovery of two Cabibbo sup-

---

[1] See http://www-focus.fnal.gov/authors.html for additional author information.

pressed decays of the D_s^+ meson; $D_s^+ \to K_S^0 \pi^- \pi^+ \pi^+$ and $D_s^+ \to K_S^0 \pi^+$. No inclusive estimates of the branching fraction for $D_s^+ \to K_S^0 \pi^- \pi^+ \pi^+$ have been reported, but several predictions exist for the branching ratio of $\frac{D_s^+ \to K_S^0 \pi^+}{D_s^+ \to K_S^0 K^+}$ [4–6]. Throughout this paper, charge conjugate modes are implied unless explicitly stated otherwise.

II. THE FOCUS EXPERIMENT

The data come from 6 billion events recorded during the 1996-1997 fixed target run at Fermilab. Electrons and positrons with an endpoint energy of approximately 300 GeV bremsstrahlung, yielding photons which interact in a segmented beryllium-oxide target to produce charmed particles. The average photon energy for events which satisfy our trigger is approximately 175 GeV. Charged particles are tracked and momentum analyzed by a system of silicon vertex detectors [7] in the target region, multi-wire proportional chambers downstream of the interaction region, and two oppositely polarized dipole magnets. Particle identification is performed by three threshold Čerenkov counters, two electromagnetic calorimeters, a hadronic calorimeter, and two muon systems. The main FOCUS trigger required tracks outside of the central region and approximately 25 GeV (or more) of energy in the hadron calorimeter.

D_s^+ decays are reconstructed using a candidate driven vertex algorithm [8]. A decay vertex is formed from the reconstructed charged tracks. The $K_S^0 \to \pi^+ \pi^-$ decays are reconstructed using techniques described elsewhere [9]. Briefly, $K_S^0 \to \pi^+ \pi^-$ decays can occur anywhere along the spectrometer. Depending on where the decays occur (upstream of the first magnet or inside the magnetic field) and on how many multi-wire proportional chambers each pion passes, the K_S^0 are given a type number and the different types vary in mass resolution and in purity. The momentum information from the K_S^0 and the charged tracks is used to form a candidate D momentum vector, which is intersected with other tracks to find the primary (production) vertex. Even though it is possible for the production vertex to be identified with a single track plus the D_s^+ momentum vector, the signal quality is greatly improved by demanding at least two primary tracks. Events are selected based on several criteria. The confidence level for the production vertex and for the charm decay vertex must be greater than 1%. The likelihood for each charged particle to be a proton, kaon, pion, or electron based on Čerenkov particle identification is used to make additional requirements [10]. We define a χ^2-like variable W_i as $-2\ln(\text{likelihood}_i)$ for the hypothesis i. In order to reduce background due to secondary interactions of particles from the production vertex, we require the decay vertex to be located outside the target material. We enhance the signal quality by cutting on the isolation variables, $Iso1$ and $Iso2$. The isolation variable $Iso1$ requires that the tracks forming the D candidate vertex have a confidence level smaller than the cut to form a vertex with the tracks from

3

the primary vertex. The isolation variable $Iso2$ requires that the tracks not assigned to the primary or secondary vertices have a confidence level smaller than the cut to form a vertex with the D candidate daughters.

III. $D_s^+ \rightarrow K_S^0 \pi^- \pi^+ \pi^+$ CHANNEL

For this channel we have excellent secondary vertex resolution with at least three charged tracks defining the vertex. We require $Iso2$ less than 1% so the secondary vertex is isolated from other tracks. We require $Iso1$ less than 1% to make sure the D_s^+ tracks do not originate at the primary vertex. The reconstructed mass of the K_S^0 must be within four standard deviations of the nominal K_S^0 mass. The typical K_S^0 mass resolution is approximately 6 MeV/c^2. For each pion candidate we require a loose cut that no alternative hypothesis is greatly favored over the pion hypothesis: $\min(W_e, W_K, W_p) - W_\pi > -5$. For the charged kaon candidate in the normalization channel we require $W_\pi - W_K > 2$. We also require the distance L ($\sim$5 mm) between the primary and secondary vertices divided by its error σ_L ($\sim$500 μm) to be at least 7. Lastly, we require an additional $D^{*+} - D^0$ cut for the $K_S^0 \pi^- \pi^+ \pi^+$ sample. The $K_S^0 \pi^- \pi^+ \pi^+$ invariant mass minus the highest $K_S^0 \pi^- \pi^+$ mass combination must be greater than 0.160 GeV/c^2. This eliminates D^{*+} background events, which simplifies the fitting function.

Figure 1(a) presents the invariant mass plot for the normalization channel $K_S^0 K^- \pi^+ \pi^+$ which is the cleanest four body D_s^+ decay containing a K_S^0. The figure contains the Cabibbo suppressed channel from the D^+ as well as the Cabibbo favored D_s^+ signal. We fit the D^+ and D_s^+ signals with Gaussians. We include a background contribution from $D^+ \rightarrow K_S^0 \pi^- \pi^+ \pi^+$ where the π^- is misidentified as a kaon and the shape is determined from a Monte Carlo simulation. The combinatoric background is fit with a 2nd degree polynomial. We find 763 ± 32 D_s^+ signal events at $L/\sigma_L > 7$. It is worth noting that this channel has been previously studied by the FOCUS Collaboration and the signal yields reported in this paper are comparable to the results already published [11].

Figure 1(b) shows the $K_S^0 \pi^- \pi^+ \pi^+$ invariant mass plot for events that satisfy the above cuts. The plot is dominated by the Cabibbo favored decay $D^+ \rightarrow K_S^0 \pi^- \pi^+ \pi^+$ while the D_s^+ signal is barely visible. Figure 1(c) is the same $K_S^0 \pi^- \pi^+ \pi^+$ invariant mass distribution in the region above the D^+ peak. The Figure 1(c) mass distribution is fit with a Gaussian with the width fixed from Monte Carlo for the signal and a first degree polynomial for the background. A signal of 179 ± 36 D_s^+ events is found from the fit.

We measure the branching fraction of the $D_s^+ \rightarrow K_S^0 \pi^- \pi^+ \pi^+$ mode relative to $D_s^+ \rightarrow K_S^0 K^- \pi^+ \pi^+$. The relative efficiency is determined by Monte Carlo simulation. The relative branching fraction is reported assuming non-resonant
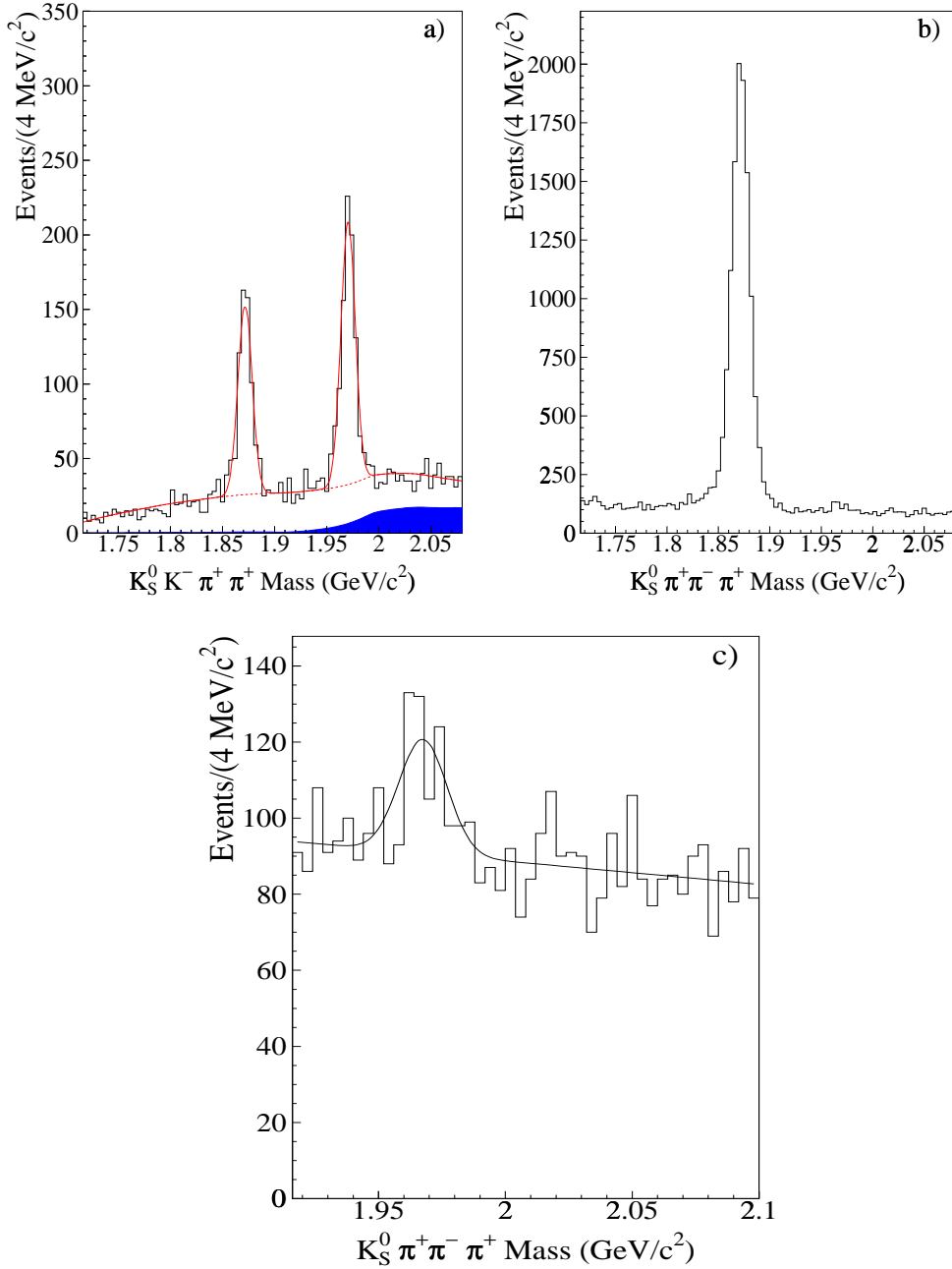
4

Fig. 1. Invariant mass distributions for (a) $K_S^0 K^- \pi^+ \pi^+$ (background reflection from a mismeasured pion from $D^+ \to K_S^0 \pi^- \pi^+ \pi^+$ is included), both the D^+ and D_s^+ signals are evident, (b) $K_S^0 \pi^- \pi^+ \pi^+$ (not fitted to show the large Cabibbo favored D^+ contribution), (c) $K_S^0 \pi^- \pi^+ \pi^+$ (with the invariant mass only plotted above the D^+ mass). The mass distribution is fit with a Gaussian with the width fixed from Monte Carlo for the D_s^+ signal and a first degree polynomial for the background.

decays for both channels. We test for dependency on cut selection in both modes by individually varying each cut. In Figure 2 we present the ratio of branching fractions for $D_s^+ \to K_S^0 \pi^- \pi^+ \pi^+$ relative to $D_s^+ \to K_S^0 K^- \pi^+ \pi^+$ as

a function of significance of separation between the primary and secondary, isolation of the secondary, and confidence level of the secondary vertex.
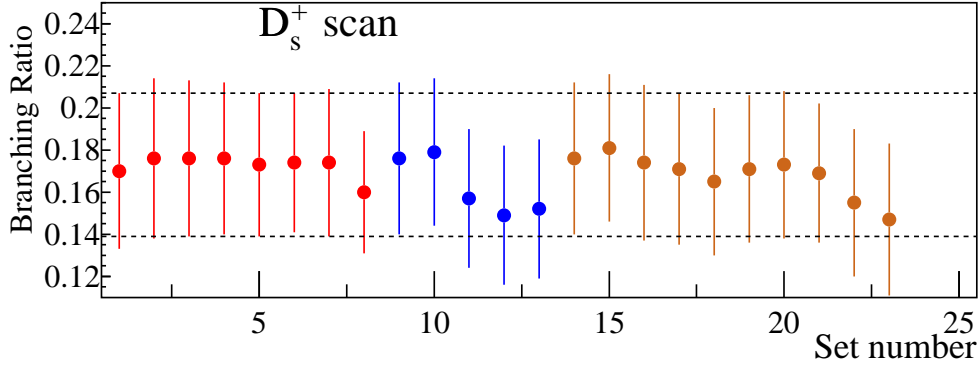

Fig. 2. The ratio of branching fractions for $D_s^+ \rightarrow K_S^0 \pi^- \pi^+ \pi^+$ relative to $D_s^+ \rightarrow K_S^0 K^- \pi^+ \pi^+$ as a function of significance of separation between the primary and secondary (first eight sets), isolation of the secondary (next five sets), and confidence level of the secondary vertex (final 10 sets).

We studied systematic effects due to uncertainties in the reconstruction efficiency, in the unknown resonant substructure, and in the fitting procedure. To determine the systematic error due to the reconstruction efficiency we follow a procedure based on the S-factor method used by the Particle Data Group [12]. For each mode we split the data sample into two independent subsamples based on D_s^+ momentum, particle versus antiparticle, decays inside the target material versus outside of target material, and on the period of time in which the data was collected. These splits provide a check on the Monte Carlo simulation of charm production, on the vertex detector (which was upgraded during the run), and on the simulation of the detector stability. We then define the split sample variance as the difference between the scaled variance and the statistical variance if the former exceeds the latter. The method is described in detail in reference [13]. We vary the subresonant states in the Monte Carlo and use the variance in the branching ratios as a contribution to the systematic error. We investigate the systematic effects based on different fitting procedures and we find this contribution to be small. The branching ratio is evaluated under various cut selection criteria, and the variance of the results is used as an additional systematic error. The systematic effects are then all added in quadrature to obtain the final systematic error. Table 1 summarizes the contributions to the systematic errors for the $\frac{\Gamma(D_s^+ \rightarrow K_S^0 \pi^- \pi^+ \pi^+)}{\Gamma(D_s^+ \rightarrow K_S^0 K^- \pi^+ \pi^+)}$ branching ratio. The result, $\frac{\Gamma(D_s^+ \rightarrow K_S^0 \pi^- \pi^+ \pi^+)}{\Gamma(D_s^+ \rightarrow K_S^0 K^- \pi^+ \pi^+)} = 0.18 \pm 0.04 \pm 0.05$, is summarized in Table 2.

IV. $D_s^+ \rightarrow K_S^0 \pi^+$ CHANNEL

This is a challenging channel to reconstruct as we typically only have a detached silicon track from the production vertex and a K_S^0 to indicate a candidate. Several criteria are used to improve the signal over background. Since

6

Table 1
Summary of the systematic error contributions for $D_s^+ \to K_S^0 \pi^- \pi^+ \pi^+$.

Contribution	$\frac{\Gamma(D_s^+ \to K_S^0 \pi^- \pi^+ \pi^+)}{\Gamma(D_s^+ \to K_S^0 K^- \pi^+ \pi^+)}$
D Momentum & Run Period	0.04
Split Target (in versus out)	0.03
Set of Cuts Selection	0.01
Fit Variance	0.01
Resonant Substructure	0.01
Total	0.05

any signal was expected to be small the selection criteria are optimized using Monte Carlo signal events and sideband background events. The figure of merit used was $S/\sqrt{B}$ and the cuts were chosen sequentially. At each step, the $S/\sqrt{B}$ distribution was determined for the full range of each cut. The cut which had the highest $S/\sqrt{B}$ was selected and a cut was made more conservative than the maximum $S/\sqrt{B}$ point. The procedure was then repeated until no further improvement was possible.

For the 90% of the K_S^0 decays that occur after the K_S^0 has passed through the silicon strip detector, we employ a specialized vertex algorithm to locate the $K_S^0 \pi^+$ vertex. We use the momentum information from the K_S^0 decay and the silicon track of the pion to form a candidate D_s^+ vector. This vector is intersected with candidate production vertices which are formed with two other silicon tracks. When the D vector is forced to originate at the production vertex, we can compute a confidence level that the D_s^+ vector formed a vertex with the charged daughter. As the type and resolution of K_S^0 is integral to finding the D_s^+ vertex, the significance of separation, L/σ_L, between the production and D_s^+ decay vertices were varied according to the K_S^0 decay type. The L/σ_L cuts varied from 7–11. This mode also required $Iso2 < 2\%$.

The normalization channel is the Cabibbo favored $D_s^+ \to K_S^0 K^+$. The selection criteria for this channel (with the exception of particle identification) are identical to $D_s^+ \to K_S^0 \pi^+$. The momentum of the D_s^+ and the charged hadron in the D_s^+ decay must be greater than 45 GeV/c and 12 GeV/c, respectively. To reduce the effect of long-lived decays and reinteractions, the proper decay time must be less than 2.5 ps with an uncertainty less than 0.12 ps. To help separate charm from combinatoric background, a momentum asymmetry cut on the two body D_s^+ decay was used: $\left| \frac{p(K_S^0) - p(h^+)}{p(K_S^0) + p(h^+)} \right| < 0.75$.

For the K^+ candidate the negative log-likelihood kaon hypothesis, $W_K = -2$ ln(kaon likelihood) must be favored over the corresponding pion hypothesis W_π by $W_\pi - W_K > 4$ while for the signal mode, the π^+ candidate must have $W_K -$

$W_\pi > -1$. The first cut serves to dramatically reduce the potentially large $D^+ \to K_S^0 \pi^+$ background which peaks at the D_s^+ mass when reconstructed as $K_S^0 K^+$ while the second cut reduces $D_{(s)}^+ \to K_S^0 K^+$ background which is smaller to begin with and peaks below the D_s^+ mass when reconstructed as $D_s^+ \to K_S^0 \pi^+$.

Fitting the $D_s^+ \to K_S^0 \pi^+$ mass plot is complicated by the presence of the large $D^+ \to K_S^0 \pi^+$ signal. Since the resolution of the state is relatively poor ($\sigma \approx 13 \, \text{MeV}/c^2$) there is very little space between the D^+ and D_s^+ peaks to estimate the background. The fit used to obtain the central value has five contributions. The first contribution is the $D^+ \to K_S^0 \pi^+$ signal which is fit with a distribution obtained from smoothing a Monte Carlo sample of reconstructed $D^+ \to K_S^0 \pi^+$ events. The mean and yield are fitted parameters. The second contribution is the $D_s^+ \to K_S^0 \pi^+$ signal which is also fit with a distribution obtained from smoothing a Monte Carlo sample of reconstructed $D_s^+ \to K_S^0 \pi^+$ events. In this case, the mean is fixed. The third and fourth contributions are reflections from $D_s^+ \to K_S^0 K^+$ and $D^+ \to K_S^0 K^+$. The reflection shapes are obtained from Monte Carlo samples of generated $D_{(s)}^+ \to K_S^0 K^+$ events reconstructed as $D_s^+ \to K_S^0 \pi^+$. The level is found by taking the same generated events, reconstructing them properly, and determining the yield. This Monte Carlo yield is then compared to the yield of the data $D_s^+ \to K_S^0 K^+$ and $D^+ \to K_S^0 K^+$ and this factor multiplies the reflection shapes. Finally, the fifth contribution is a quadratic polynomial to account for generic combinatorial background.

The $K_S^0 K^+$ mass plot is also fit with five contributions. The $D_s^+ \to K_S^0 K^+$ and $D^+ \to K_S^0 K^+$ are fit with functions obtained from smoothing reconstructed Monte Carlo samples. The masses and yields are fitted in both cases. The reflection from $D^+ \to K_S^0 \pi^+$ is also obtained from Monte Carlo and fixed based on the number of reconstructed $D^+ \to K_S^0 \pi^+$ events in data. The fourth contribution, a reflection from $D_s^+ \to K_S^0 K^+ \pi^0$ is allowed in the fit. The shape is obtained from Monte Carlo simulation but the level is allowed to vary in the fit since the branching ratio is poorly known and we do not have a fully reconstructed sample available. As before, the fifth contribution is generic combinatoric background which is modeled with a quadratic polynomial.

From the $K_S^0 \pi^+$ fit shown in Fig. 3 we obtain a D_s^+ yield of 113 ± 26 events. The $K_S^0 K^+$ fit presented in Fig. 3 gives a yield of 777 ± 36 D_s^+ events and the number of events found for the $D_s^+ \to K_S^0 K^+ \pi^0$ reflection is consistent with PDG branching ratios and our efficiency.

The systematic uncertainties are divided into cut variants and fit variants. In both cases the systematic uncertainty is obtained from the square root of the standard deviation of the values weighted by the individual uncertainty. The actual procedure is as follows. For each variant (but not the default), the branching ratio BR_i is calculated along with the uncertainty σ_i. The average,
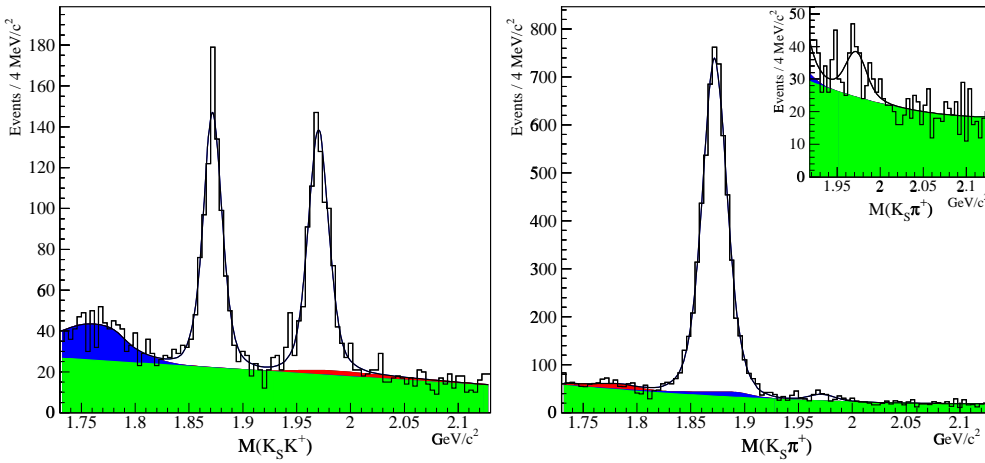
8

Fig. 3. Invariant mass distributions for $K_S^0 K^+$ (left) and $K_S^0 \pi^+$ (right). The fits are over the entire mass range. Most of the background is modeled by a quadratic polynomial. The remaining background is due to reflections and is a different shade. The $K_S^0 K^+$ mode has a large reflection component from $D_s^+ \to K_s^0 K^+ \pi^0$ below the D^+ peak and a small reflection component from $D^+ \to K_s^0 \pi^+$ under the D_s^+ peak. The $K_s^0 \pi^+$ has small reflection contributions below (under) the D^+ peak from $K_S^0 \pi^+$ decays from D^+ (D_s^+). All signal and reflection shapes come from a Monte Carlo simulation.

weighted by the inverse of the square of the uncertainty, is calculated

$$\overline{BR} \; = \; \frac{\sum_i \frac{BR_i}{\sigma_i^2}}{\sum_i \frac{1}{\sigma_i^2}}. \tag{1}$$

The systematic uncertainty is obtained from the square root of the standard deviation which comes from a "weighted" χ^2:

$$\sigma_{\text{sys}} \; = \; \sqrt{\frac{\sum_{i=1}^{N} \left(\sigma_0^2 \frac{BR_i - \overline{BR}}{\sigma_i^2} \right)^2}{N-1}} \tag{2}$$

where σ_0 is the uncertainty on the default measurement.

For each of the cut variants, both the $D_s^+ \to K_S^0 \pi^+$ and $D_s^+ \to K_S^0 K^+$ samples are changed the same (with the exception of particle identification cuts). The variations are consistent with statistical fluctuations and the systematic uncertainty is determined from the standard deviation which is dominated by the $D_s^+ \to K_S^0 \pi^+$ variations. The systematic uncertainty from the cut variant is $\sigma_{sys}^{cut} = 0.010$.

The systematic uncertainty in estimating the yield of $D_s^+ \to K_S^0 K^+$ events is negligible compared to estimating the yield of $D_s^+ \to K_S^0 \pi^+$ events. Therefore, for the fit variants we vary how the $K_S^0 \pi^+$ mass plot is fitted. Some of the variations include fitting with a Gaussian, allowing the mass and width to

9

float, and fitting only above the D^+ mass peak. The variation in the $D_s^+ \to K_S^0 \pi^+$ yield, again weighted by the uncertainty squared, gives the systematic uncertainty. The systematic uncertainty on the yield from the fit variations is 9.0 events which corresponds to a relative uncertainty of 8.0% and translates into a systematic uncertainty on the branching ratio of $\sigma_{sys}^{fit} = 0.008$. Adding the cut and fit systematic uncertainties in quadrature gives a total systematic uncertainty on the branching ratio of 0.013.

V. SUMMARY OF RESULTS

In conclusion we have presented the first evidence of the Cabibbo suppressed decay mode $D_s^+ \to K_S^0 \pi^- \pi^+ \pi^+$ and measured the relative branching ratio of $\frac{\Gamma(D_s^+ \to K_S^0 \pi^- \pi^+ \pi^+)}{\Gamma(D_s^+ \to K_S^0 K^- \pi^+ \pi^+)} = 0.18 \pm 0.04 \pm 0.05$. A naive expectation for this branching ratio is $\tan^2\theta_C = 0.054$. Compared with this expectation the branching ratio is more than 3 times larger. One contributing factor is there is more phase space available in the $D_s^+ \to K_S^0 \pi^- \pi^+ \pi^+$ decay than in the $D_s^+ \to K_S^0 K^- \pi^+ \pi^+$ decay. Another factor is that the K_S^0 in the denominator of the ratio comes from a $\overline{K^0}$. In the numerator the K_S^0 may be the result of either a $\overline{K^0}$ or a K^0 decay. Perhaps a better understanding of this ratio would result from reporting the ratio $\frac{\Gamma(D_s^+ \to K_S^0 \pi^- \pi^+ \pi^+)}{\Gamma(D_s^+ \to K_S^0 K^- \pi^+ \pi^+) + \Gamma(D_s^+ \to K_S^0 K^+ \pi^+ \pi^-)}$. Using the branching ratio reported in reference [11] for $\frac{\Gamma(D_s^+ \to K_S^0 K^+ \pi^+ \pi^-)}{\Gamma(D_s^+ \to K_S^0 K^- \pi^+ \pi^+)} = 0.586 \pm 0.052 \pm 0.043$ we find $\frac{\Gamma(D_s^+ \to K_S^0 \pi^- \pi^+ \pi^+)}{\Gamma(D_s^+ \to K_S^0 K^- \pi^+ \pi^+) + \Gamma(D_s^+ \to K_S^0 K^+ \pi^+ \pi^-)} \approx 0.11$.

We also present evidence for $D_s^+ \to K_S^0 \pi^+$ and measure its branching fraction relative to $D_s^+ \to K_S^0 K^+$: $\frac{\Gamma(D_s^+ \to K_S^0 \pi^+)}{\Gamma(D_s^+ \to K_S^0 K^+)} = 0.104 \pm 0.024 \pm 0.013$. This branching ratio is also larger than $\tan^2\theta_C$, but is slightly smaller than predictions [4–6] which range from 14% to 17%. The results are summarized in Table 2.

Table 2
Branching ratios, event yields, and efficiency ratios for modes involving a K_S^0. All branching ratios are inclusive of subresonant modes.

Decay Mode	Ratio of Events	Efficiency Ratio	Branching Ratio
$\frac{\Gamma(D_s^+ \to K_S^0 \pi^- \pi^+ \pi^+)}{\Gamma(D_s^+ \to K_S^0 K^- \pi^+ \pi^+)}$	$\frac{179 \pm 36}{763 \pm 32}$	1.34	$0.18 \pm 0.04 \pm 0.05$
$\frac{\Gamma(D_s^+ \to K_S^0 \pi^+)}{\Gamma(D_s^+ \to K_S^0 K^+)}$	$\frac{113 \pm 26}{777 \pm 36}$	1.39	$0.104 \pm 0.024 \pm 0.013$

VI. ACKNOWLEDGEMENTS

References

[1] J. M. Link et al. (FOCUS Collaboration), Phys. Lett. **B 601**, 10 (2004).

[2] P. L. Frabetti et al. (FNAL E687 Collaboration), Phys. Lett. **B 359**, 403 (1995).

[3] J. M. Link et al. (FOCUS Collaboration), Phys. Lett. **B 541**, 227 (2002).

[4] R. C. Verma and A. N. Kamal, Phys. Rev. **D 43**, 829 (1991).

[5] F. Buccella, M. Lusignoli, G. Miele, A. Pugliese, and P. Santorelli, Phys. Rev. **D 51**, 3478 (1995).

[6] F. Buccella, M. Lusignoli, and A. Pugliese, Phys. Lett. **B 379**, 249 (1996).

[7] J. M. Link, et al. (FOCUS Collaboration), Nucl. Instrum. Meth. **A 516**, 364 (2004).

[8] P. L. Frabetti et al. (FNAL E687 Collaboration), Nucl. Instrum. Meth. **A 320**, 519 (1992).

[9] J. M. Link et al. (FOCUS Collaboration), Nucl. Instrum. Meth. **A 484**, 174 (2001).

[10] J. M. Link et al. (FOCUS Collaboration), Nucl. Instrum. Meth. **A 484**, 270 (2002).

[11] J. M. Link et al. (FOCUS Collaboration), Phys. Rev. Lett. **87**, 162001 (2001).

[12] W.-M. Yao et al. (Particle Data Group), J. Phys. **G 33**, 1 (2006).

[13] J. M. Link et al. (FOCUS Collaboration), Phys. Lett. **B 555**, 167 (2003).